06

Effect of nanodiamonds with different surface states on ion channel packing and proton conductivity of composite perfluorosulfone membranes

© V.T. Lebedev,[1] Yu.V. Kulvelis,[1] O.N. Primachenko,[2] A.S. Odinokov,[3] E.A. Marinenko,[2] A.V. Shvidchenko,[4] A.I. Kuklin,[5] O.I. Ivankov[5]

[1] St. Petersburg Nuclear Physics Institute, National Research Center Kurchatov Institute, 188300 Gatchina, Russia
[2] Institute of Macromolecular Compounds, Russian Academy of Sciences, 199004 St. Petersburg, Russia
[3] Russian Scientific Center „Applied Chemistry“, 193232 St. Petersburg, Russia
[4] Ioffe Institute, 194021 St. Petersburg, Russia
[5] Frank Neutron Physics Laboratory, Joint Institute for Nuclear Research, 141980 Dubna, Moscow oblast, Russia
e-mail: lebedev_vt@pnpi.nrcki.ru

Received September 26, 2024
Revised September 26, 2024
Accepted September 26, 2024

A copolymer of the Aquivion® type was modified with detonation diamonds (size 4−5 nm, concentration 0.25−5.0 wt.%) and studied using neutron scattering, measuring the packing period of ion channels in the matrix. Positively charged diamonds with a hydrogen-saturated surface at a concentration of 0.5 wt.% provided a 30 % increase in the ionic conductivity of the membranes at a temperature of 50 °C due to compaction of the packing of channel assemblies. Due to the electrostatic attraction of the components, a more developed conductive diamond-copolymer interface was created in such membranes than in composites with negatively charged ionic groups of the components. When the matrix was filled with hydrophobic fluorinated diamonds (1 wt.%), a fivefold decrease in ionic conductivity was observed due to the disruption of the connectivity of ion channels. The found correlations between the structure and ionic conductivity of the composites depending on the type and amount of filler are important for the targeted formation of membranes upon modification with nanoparticles.

Keywords: membranes, diamonds, conductivity, structure.

DOI: 10.61011/TP.2025.02.60813.287-24

Introduction

To improve the functional properties of ion-exchange membranes of chemical fuel elements, promising approaches are offered to modify Nafion® and Aquivion® type original perfluorinated copolymers with nanoparticles that form a conductive interface with copolymer and reinforce the copolymer for improvement and stabilization of stress-strain and conductive properties of materials [1–26].

However, it is important to ensure interaction between the filler and exactly the polar macromolecule fragments (terminal ion groups of side chains) to improve coherence and transport properties of the matrix ion channel network by integrating nanoparticles into it. For this, hydrophilic particles are used, in particular, inorganic oxide-based particles (SiO_2, TiO_2, ZrO_2) [1–4]. Thus, in Nafion matrix composite materials, ~ 5 nm SiO_2, ZrO_2 particles, having a minimum influence on crystallinity and structure, increased the material's water-retaining capability and conductivity at high temperature [2]. The authors [3] introduced the ZrO_2-TiO_2 particles into the Nafion membrane to optimize their fractions (Zr:Ti = 1:3). Thus, the weight of absorbed water was increased and electrochemical parameters of the Nafion112 matrix were exceeded in the operating conditions at 120 °C, relative humidity of 50% (RH) and pressure of 2 atm. It was found that the SiO_2, TiO_2, ZrO_2 particles introduced into the Nafion matrix, while reducing the conductivity at low temperatures, increased the conductivity during heating in low moisture content conditions, which is important for membrane applications. ZrP particles help keep the conductivity at high RH values and enhance it as the temperature increases and RH decreases [4]. To retain water in composite materials, the porous structure of filler particles was important, that ensured the conductivity growth with respect to the original matrix [4].

Carbon structures (fullerenes, nanotubes, nanodiamonds, graphene and derivatives) with grafted atoms and polar groups (H, F, OH, COOH, etc.) are of particular interest for rendering hydrophilic properties to these objects [27–34] to form hybrid ion channels that involve these groups and sulfonic acid groups of the matrix, and to improve the stress-strain properties of matrices [4,35–38].

Generally, through small nanoparticle fractions, the degree of water saturation and proton conductivity of membranes may be increased considerably with fuel crossover reduction, moreover, at high temperatures that are required for effective operation of polyelectrolyte fuel cells [4,38–40].

A considerable positive effect was achieved when nanotubes, graphenes and nanodiamonds [41–46], that differed in dimensions and constituted extended linear (1D), planar (2D) and compact globular (3D) objects, were introduced into the perfluorinated matrices. Among them, detonation nanodiamonds (DND, size 4−5 nm) are most comparable with the scales of ion channels and small pores for proton migration in perfluorinated membranes. When particles have a hydrophilic surface, this factor is favorable for diamond integration into the polymer channel network without serious damage to the matrix structure formed after segregation of ion groups lining the ion channel surface in hydrophobic skeleton polymer chain shells [47,48].

Structural interpretation of Nafion and Aquivion type perfluorinated copolymers with similar chemical composition and different length of side chains containing sulfonic acid groups on the ends provided construction of models based on the electron microscopy, neutron and synchrotron scattering (SANS, SAXS) data that indicated formation of fibrillar (lamellar) ion channels and nanoscale pores [49–61].

The models rely mainly on the SANS and SAXS experiment data demonstrating the interference scattering peaks (ionomer peaks) that reflect the cylindrical ion channel packaging with a period of ~ 3 nm [52–61]. Thus, the membranes have channel assemblies (bundles) via which protons are transported [58]. This kind of equilibrium ordered channel structure is formed as a result of membrane annealing at $\sim 100-120\,^{\circ}$C [40].

At the same time membrane filling with nanoparticles, for example, diamonds, disturbs the original polymer matrix structure where ionomer peak shift, amplitude and width variation are observed [62], i.e. significant structural changes that affect the material's proton conductivity. Depending on the physical and chemical properties and modifier fraction, the conductivity may increase or decrease [62].

Correlation between the type of ordering and conductive properties of perfluorinated diamond-filled copolymers is poorly known quantitatively, which prevents from complete understanding of the mechanisms of action of various diamond modifiers on composite structure and electrophysical properties and identifying their correlation.

An objective of this study was to find and identify the type of correlations between the ion channel structure data and conductive properties of composite membranes with hydrophilic diamonds of different surface potential signs and, for comparison, with hydrophobic diamonds interacting mainly with nonpolar copolymer chains without formation of a conductive interface.

1. Samples and research methods

1.1. Perfluorinated copolymers

Composites were prepared using a Aquivion® type material. It was synthesized by the water-emulsion method [63] with perfluorinated monomer copolymerization (perfluoro-3-oxapentensulfonyl fluoride) with tetrafluoroethylene (TFE, 0.7−1.3 MPa) in thermostating conditions (40−60 °C) in a steel reactor (0.45 l, horseshoe agitator). TFE was fed into a sulfonyl fluoride monomer emulsion stabilized with perfluorinated surfactant (ammonia perfluorononanoate). Copolymer with an equivalent chain weight (EW) of 890 g/mol (equivalent to the ion group $-SO_3H$) had a proton conductivity of 0.15 S/cm with equilibrium (maximum) water content of 37.0 wt.% (20 °C).

1.2. Nanodiamond hydrosols

Diamonds (DND, $d_p \approx 4.5$ nm, dispersion $\Delta d_p/d_p \approx 50\%$) were produced by detonation synthesis (FGUP SKTB Tekhnolog, Saint Petersburg, Russia), then deagglomeration (annealing, ultrasonic dispersion) and chemical cleaning (acid etching) were performed [64–66]. By removing graphene-like fragments from the particle surfaces, single-phase diamond crystals were fabricated [65,66]. They formed stable hydrosols (~ 1 wt.%) with adjustable particle surface potential ($\sim 30-70$ mV) — positive (DNDZ+), if they were preliminary annealed in hydrogen flow (500 °C) with H-, OH-group grafting, or negative (DNDZ-) when annealed in air (430 °C) with COOH-group grafting [64,65]. Particles were mixed with deionized water, subjected to ultrasonic treatment, and were centrifugated to separate fine fractions [64].

In addition to the DNDZ- and DNDZ+ diamonds, fluorinated DNDF diamonds were prepared by annealing in F_2 (450 °C) atmosphere that reacted with the surface particle groups (C−OH, C−H, C=O, COOH), and decomposition of the groups gave rise to C-F bonds (fluorine substitution of 97% of hydrogen atoms) [30,67,68]. Raw detonation nanodiamonds (TU 2-037-677-94) made by Zababakhin Russian Federal Nuclear Center (RFNC VIIF), Snezhinsk, Russia) were used as a starting material. DNDF powders produced stable sols in dimethylformamide (DMFA, (0.17 wt.%) with ~ 4.5 nm particles (negative potential) and ~ 20 nm scale aggregates according to the dynamic light scattering data (Zetasizer Nano ZS analyzer, Malvern Instruments Ltd.).

1.3. Membranes

Membrane films were fabricated by the flow coating method [69]. Copolymer in the $-SO_3Li$-form dissolved in DMFA was applied to a heated glass substrate. After fabrication of the film from solution, the film was converted into the $-SO_3H$-form by washing with 15% nitric acid to transform the film to a proton-conductive membrane [69]. For synthesis of composite materials, DMFA-dispersed

diamonds were added to the copolymer solution (2 wt.%) to make $\sim 50\,\mu$m films with the fractions of diamonds equal to 0.25–5.0 wt.% [69]. The films were converted from the $-SO_3Li$-form to $-SO_3H$-form by acid washing.

1.4. Research methods

Procedure for preparing and study of modified membranes and diamond components combined a set of structural, physical and chemical methods (electron and atomic-force microscopy, dynamic light and neutron scattering, stress-strain property, conductivity, water adsorption measurement, etc.) that are addressed in [29–31,40,46–48,62,63,65–69]. This study was focused on the search for correlation between the ion channel structures and composite membrane conductivity depending on the type and number of diamond modifiers. Therefore, comparative analysis of data obtained by the conductometry and small-angle neutron scattering (SANS) methods was mainly carried out. Proton conductivity of samples with equilibrium (maximum) watering (30–33 wt.%, boiling at 100 °C, 1 h) was measured by the standard impedance spectroscopy method at 20 and 50 °C (Z-3000X unit, 4-electrode measurement cell connection diagram, frequency range 10–150 000 Hz, Elins, Russia). Structure of dry samples (20 °C) was examined by the SANS method (YuMo spectrometer, IBR-2 reactor, Joint Institute for Nuclear Research, Dubna) [70] by measuring the intensities of scattered neutrons by angles (θ) with momentum transfers $q = (4\pi/\lambda)\sin(\theta/2) = 0.05–6.0\,\text{nm}^{-1}$ for the spectrum of $\lambda \sim 0.05–0.8$ nm neutrons falling on the sample [71]. After background subtraction, data calibration was performed using a standard (vanadium sample) being incoherent scatterer for neutrons. SAS software package [72] was used to find absolute scattering cross-sections of the samples $d\Sigma(q)/d\Omega$ were found depending on the momentum transfer (q) per unit of solid angle equivalent to cm^3 of the sample volume. Then, the neutron scattering and object modeling data interpretation procedure was used [73].

2. Results and discussion

2.1. Neutron investigations of membranes

During neutron experiments on dry membranes with DNDZ+, DNDZ-, DNDF particles, considerable growth of the scattering cross-section $\sigma(q)$ was observed in the region of the momentum transfers $q \sim 0.01–1.0\,\text{nm}^{-1}$ with increasing fraction of filler (0.25–5.0 wt.%) due to a high contrast of dense diamond crystals with respect to the polymer matrix, which is illustrated by the data for the matrix and composite materials with the typical diamond concentration of $C = 0.5$ wt.% (Figure 1).

Behavior of the cross-sections $\sigma(q) \sim q^{-Df}$ indicates that diamonds in the polymer matrix as well as in liquid dispersions [74,75] are arranged in mass fractal type structures

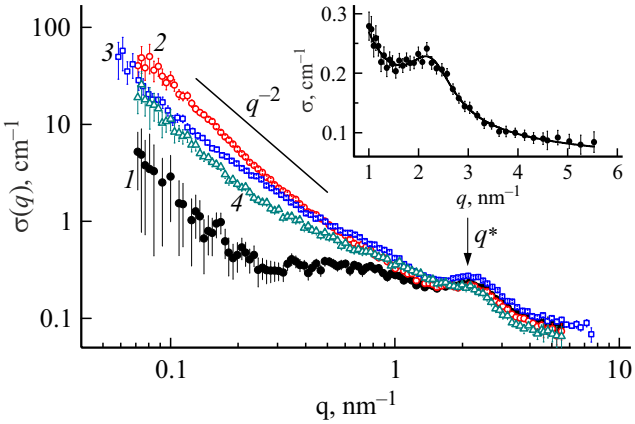

Figure 1. Neutron scattering cross-sections $\sigma(q)$ in membranes depending on the momentum transfer: *1* — original copolymer, *2–4* — composite materials with 0.5 wt.% of the DNDZ+, DNDZ-, DNDF diamonds. Ionomer peak position (q^*) is shown. The line shows typical behavior of the cross-sections $\sim q^{-2}$. Inset — example of peak approximation by the Lorentz function, data (1).

with dimension $D_f \sim 2$, i.e. they are chain (branched) particle aggregates (Figure 1).

Diamonds that differ in chemical properties and degree of hydrophilic property of the surface due to the grafted groups demonstrate common structuring patterns in the matrix polymer where they produce chain (reinforcing) scaffolds.

However, diamonds affect the order of bundled conductive ion channels differently, which is expressed in the presence of an interference maximum (ionomer peak) on the cross-section curves in the position $q^* \sim 2\,\text{nm}^{-1}$ corresponding to the channel packaging period in the bundles, $L_C = 2\pi/q^* \sim 3$ nm (Figure 1). For the series of samples with the DNDZ+, DNDZ-, DNDF diamonds, ionomer peak parameters (position of the maximum $q^* = q_m$, amplitude A_m and width Γ) (Figure 2) were found from the data approximation by the Lorentz function multiplied by the squared form-actor of thin linear channels ($1/q$) (Figure 1) less the contributions of scattering from the channels separately and from diamonds

$$\sigma(q) = (A_m/q)\left[1 + (q - q_m)^2/\Gamma^2\right]^{-1}. \qquad (1)$$

Growth of the modifier fraction causes the peak amplitude reduction that is strongly pronounced when fluorinated diamonds are introduced into the matrix, but is displayed to a lesser extent when the matrix is filled with the DNDZ+, DNDZ- particles (Figure 2, *a*).

DND-F diamonds, by contacting mainly with hydrophobic skeleton chains in the channel shells, disturb the channel packaging even in minimum amounts (0.25 wt.%) where, due to the growth of the channel packaging period (L_C), the ionomer peak shifts towards lower momentum transfers (Figure 2, *b, d*). At the same time, when the peak is getting narrow, Γ/q_m and, consequently, the aggregation number

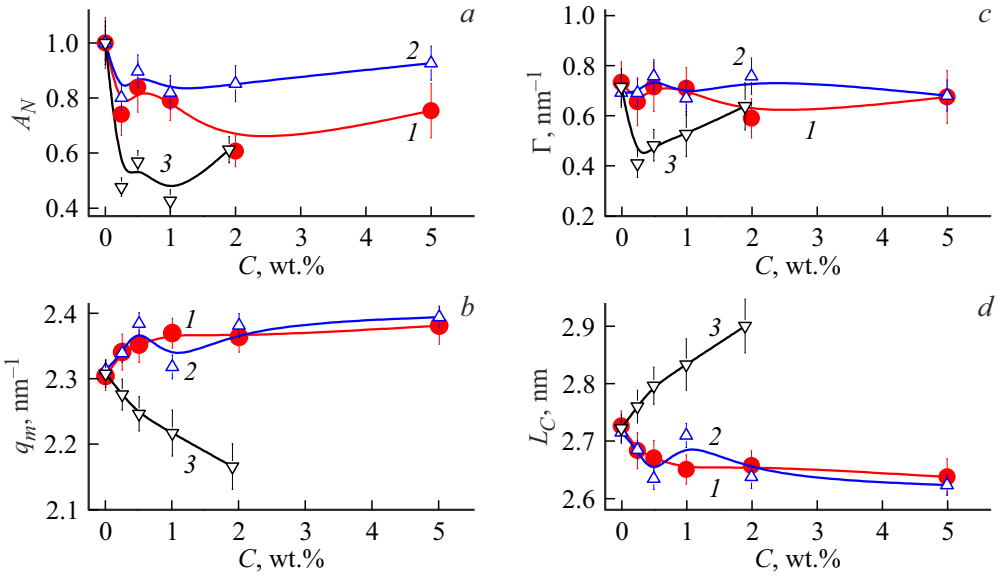

Figure 2. Ionomer peak parameters depending on the concentration (C) of the DNDZ+, DNDZ-, DNDF diamonds (1–3): a, b — amplitude A_m and width Γ; c, d — maximum q_m position, channel packaging period L_C.

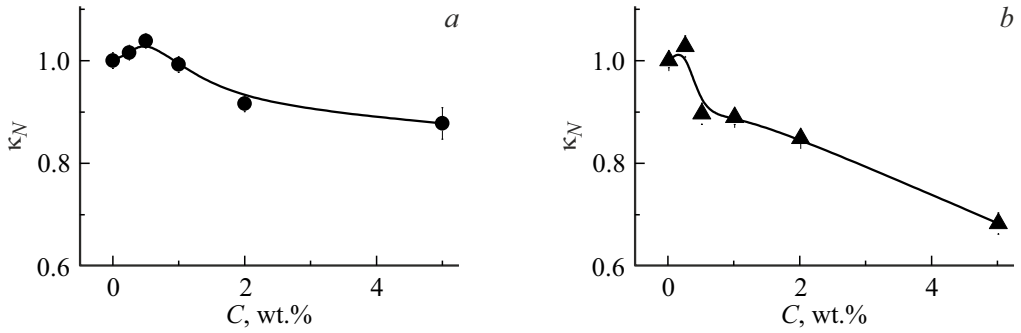

Figure 3. Normalized proton conductivity (20 °C) of composite materials $\kappa_N = \kappa(C)/\kappa(C = 0)$ depending on the fraction of the DNDZ+, DNDZ- diamonds (a, b).

of channels in bundles are retained, i.e. channel assembly disintegration doesn't occur.

DNDZ+, DNDZ- diamonds with strong hydrophilic properties, by interacting more with polar chain fragments, cause channel assembly compression. This can be seen from the peak shift towards higher momentum transfers, which indicates reduction of the channel packaging period (Figure 2, b, d).

However, curves $L_C(C)$ differ qualitatively when different diamonds are introduced in the matrix (Figure 2, d). Modification by positively charged DNDZ+ diamonds causes monotonous reduction of the period by $\Delta L_C/L_C(C = 0) \sim 3\%$ (Figure 2, d). For negatively charged DNDZ- diamonds, reduction of the period ($C = 0$–0.5 wt.%) is changed by its sharp growth upon reaching the concentration $C = 1$ wt.% followed by decrease at $C > 1$ wt.% (Figure 2, d).

As the DNDZ+ diamonds were added to the matrix, the mutual attraction of oppositely charged components facilitates compact channel packaging in the assemblies (bundles), but upon reaching the diamond concentration $C^* \sim 1$ wt.%, this resource gets depleted and a slight reduction of the period at $C > C^*$ means compression of ion channels $\Delta L_C/L_C(C = 0) \sim 0.5$ wt.% (Figure 2, d). $C^* \sim 1$ wt.% is corresponded by numerical diamond concentration $N_D \approx 1.2 \cdot 10^{17}\,\mathrm{cm}^{-3}$, where the mean spacing between them $R_{int} = N_D^{-1/3} \approx 20$ nm decreases to the size of polymer domains with ordered (crystalline) skeleton chain layout [48], and diamonds fill the rarefied areas at the domain boundaries.

In composites with DNDZ-, mutual repulsion of like-charged components prevails, and their segregation is probable, which is followed by compaction of channel assemblies at low content of the filler ($C \leq 0.5$ wt.%). However, upon reaching the critical point $C^* \sim 1$ wt.%, diamond particles at the domain boundaries loosen the chain packaging in them. The channels and their polymer shells get expanded in the same proportion, and the channel packaging period is restored almost to the initial level , but further increase in the diamond concentration ($C \geq 2$ wt.%)

leads to ion channel compression and packaging period reduction (Figure 2, *d*).

2.2. Structure and proton conductivity of membranes

Channel restructuring under the action of diamonds is directly reflected in the ion conductivity behavior $\kappa_N = \kappa(C)/\kappa(C=0)$ (Figure 3) that grows initially, $\kappa_N \sim L_C^{-2}$, due to channel assembly compaction (with constant channel diameter), but then decreases, $\kappa_N \sim (L_C - 2\delta_S)^2$, due to channel compression in the polymer shells with constant thickness δ_S.

When the matrix is filled with the DNDZ+ diamonds, the conductivity first increases by $\sim 4\%$ ($C = 0-0.5$ wt.%) and then decreases by 10% ($C = 1-5$ wt.%) with respect to the level for the matrix (Figure 3, *a*). The first segment reflects the channel assembly compaction that stimulates the conductivity, the second segment corresponds to the channel compression and conductivity reduction (Figure 3, *a*). DNDZ- diamonds help increase the conductivity only at the minimum concentration (0.25%) causing further decrease in conductivity (Figure 3, *b*).

Data analysis for the composite materials with DNDZ+ has confirmed the correlations between the normalized conductivity and period $L_N = L_C/L_C(C=0)$ according to $\kappa_N^{1/2} = P_1/L_N$, $\kappa_N^{1/2} = P_2(L_N - P_3)$ in the diamond concentration intervals $C = 0-0.5$, $0.5-5.0$ wt.%, respectively (Figure 4).

The following parameters were found from the linear data approximation (Figure 3): $P_1 = 0.995 \pm 0.002$, $P_2 = 5.95 \pm 3.12$, $P_3 = 0.81 \pm 0.09$.

$P_1 \approx 1$ shows that the membrane conductivity, $\kappa_N \approx 1/L_N^2$, defined by the proton transfer in the bundled ion channels grows proportionally to the number of channels per unit of bundle cross-section when the assemblies are compacted by small amounts of diamonds ($C = 0-0.5$ wt.%), that don't cause ion channel compression (Figure 4). The latter occurs when the matrix is filled with diamonds ($C \geq 0.5$ wt.%), when conductivity decreases proportionally to the squared channel diameter $d_I = (L_C - 2\delta_S)$ according to $\kappa_N = P_2^2(L_N - P_3)^2$, where $L_N = L_C/L_C(C=0)$ is the normalized diameter with $P_3 = 2\delta_S/L_0$ that is defined by the thickness (δ_S) and external diameter $L_0 = L_C(C=0)$ of the shell in the original matrix and is equal to the channel packaging period (Figure 4). According to P_3 and L_0, the shell thickness is $\delta_S = P_3 L_0/2 = 1.1 \pm 0.1$ nm, and the ion channel diameter is equal to $d_I = (L_0 - 2\delta_S) = 0.5 \pm 0.2$ nm in line with the neutron scattering data in such membranes [76]. As the membranes are getting enriched with diamonds, the channel packaging period decreases due to compression of the ion channels whose diameter decreases by $\sim 20\%$ up to $d_I = L_C - 2\delta_S = 0.4 \pm 0.2$ nm with the diamond fraction of $C = 5$ wt.%.

Unlike composite materials with DNDZ+ particles charged oppositely to the matrix, when their mutual attraction stabilizes the channel network, in membranes with like-charged components with DNDZ- $C \geq 0.5$ wt.%, loosening of the channel assemblies causes conductivity reduction (Figure 3, *b*) according to the correlations between $\kappa_N^{1/2}$ and L_N (Figure 5).

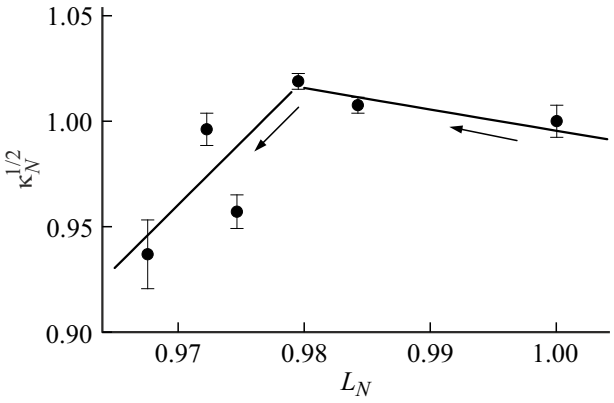

Figure 4. Linear correlations between conductivity data $\kappa_N^{1/2}$ (20 °C) and normalized packaging periods L_N of ion channels in composite materials with the DNDZ+ diamonds.

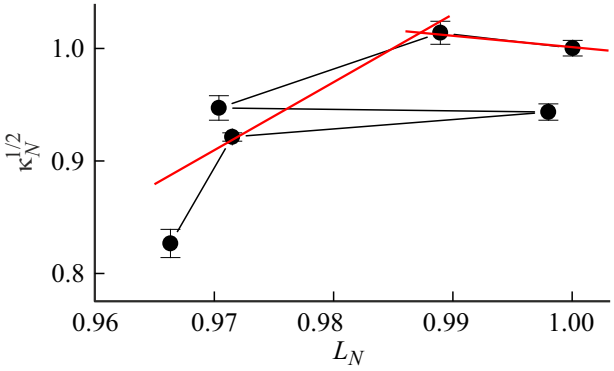

Figure 5. Correlations between the conductivity data $\kappa_N^{1/2}$ (20 °C) and normalized channel packaging periods L_N in composite materials with the DNDZ- diamonds. Linear approximation functions are plotted.

In the matrix with increasing amount of DNDZ- (0–0.5 wt.%), $\kappa_N^{1/2}$ varies approximately as in composite materials with DNDZ+, but the assembly packaging concentration interval is limited by a small fraction of diamonds ($C = 0.25$ wt.%), where the channel packaging period is reduced only by $\Delta L_N \sim 1\%$ (Figure 5). As the concentration increases to $C = 0.5$ wt.%, channel compression with period reduction by $\Delta L_N \sim 3\%$ takes place (Figure 5). However, when $C^* = 1$ wt.%, the effect is inverted with the period jump $\Delta L_N \sim 3\%$ almost to the value as that of the matrix (Figure 5). In the critical point ($C^* = 1$ wt.%), as when the matrix is filled with DNDZ+ particles, the mean spacing between them $R_{int} \sim 20$ nm decreases to the size of polymer domains observed in scattering with momentum transfers $q \sim 0.3-0.8\,\text{nm}^{-1}$ (Figure 1, data *1*). In these conditions, due to repulsion of like-charged ion groups of

the matrix and DNDZ-, the chain packaging is damaged, the channels and shells are expanded in the same proportion, therefore the conductivity doesn't vary significantly (Figure 5). It is important that, when $C \geq C^*$, segregation with formation of nanoscale aggregates is typical of the DNDZ- diamonds [47]. Then the diamond-depleted channel structures change to subcritical state which was observed with $C \geq 2$ wt.%, when the channel packaging period was reduced again ($\Delta L_N \sim 3\%$) with a small decrease in the conductivity, but it decreased significantly with the excess of diamonds ($C = 5$ wt.%) that prevented from arranging the copolymer ion groups into channel structures (Figure 5).

In the DNDZ- diamond concentration ranges $C = 0-0.25$ and $0.25-5.0$ wt.%,correlations between $\kappa_N^{1/2}$ and L_N in the membranes as well as in the samples with DNDZ+ are characterized by $\kappa_N^{1/2} = P_1/L_N$, $\kappa_N^{1/2} = P_2(L_N - P_3)$ with $P_1 = 1.001 \pm 0.001$, $P_2 = 6.1 \pm 2.5$, $P_3 = 0.82 \pm 0.06$ (Figure 5). They are not much different from the parameters for the matrix filled with the DNDZ+ diamonds because in both cases there is a common mechanism of ion group segregation from nonpolar copolymer chains.

Using P_3, shell thickness $\delta_S = P_3 L_0/2 = 1.1 \pm 0.1$ nm and ion channel diameter $d_I = (L_0 - 2\delta_S) = 0.5 \pm 0.2$ nm were found in the original diamond-free membrane. These quantities agree with those for the matrix in the sample series with DNDZ+. Copolymer saturation with DNDZ- particles ($C = 5$ wt.%), as the DNDZ+ diamond filling case, caused channel compression by $\sim 20\%$ to $d_I = L_C - 2\delta_S = 0.4 \pm 0.1$ nm.

The established patterns of unlike-charged diamond influence on the conductive ion channel packaging and sizes are common. Their influence on the membrane conductivity is displayed more vividly during heating of composite materials, which activates proton transfer.

At 50 °C, the growth of conductivity by $\sim 30\%$ was achieved in the composite materials due to the DNDZ+ diamonds and exceeded the effect of DNDZ- ($\sim 10\%$) (Figure 6).

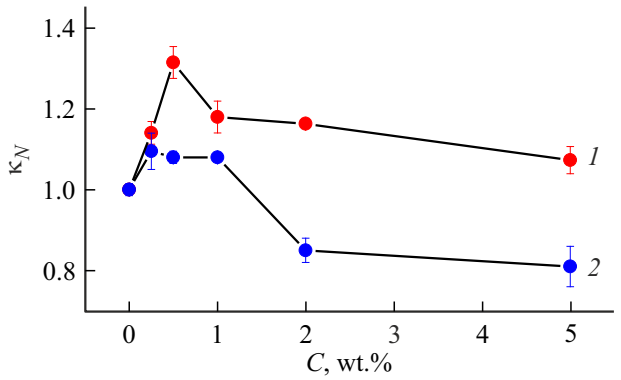

Figure 6. Normalized proton conductivity $\kappa_N = \kappa(C)/\kappa(C = 0)$ of composite materials at 50 °C depending on the fraction of the DNDZ+, DNDZ- (*1, 2*).

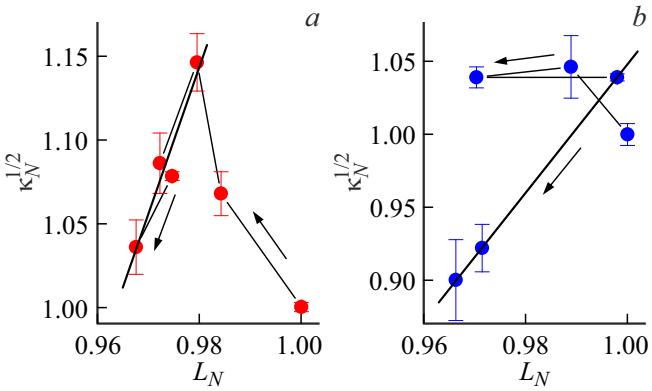

Figure 7. Correlations between the conductivity data $\kappa_N^{1/2}$ and channel packaging periods L_N for membranes with the DNDZ+ and DNDZ- diamonds at 50 °C (*a, b*). Concentration growth directions are designated. Linear data approximation in the concentration ranges (L_N) where diamonds cause channel compression.

Correlation analysis results between the conductivity at 50 °C and channel structure data are shown in Figure 7. As the heated composite materials were enriched with the DNDZ+ diamonds ($C = 0-5$ wt.%), they demonstrated the dependence of $\kappa_N^{1/2}$ on L_N similar to that at 20 °C (Figure 4, 7, *a*). $\kappa_N^{1/2}$ first increased, then decreased linearly with period reduction $\kappa_N^{1/2} = P_2(L_N - P_3)$ with $P_2 = 8.8 \pm 1.8$, $P_3 = 0.85 \pm 0.03$ (Figure 7, *a*). The found channel shell thickness $\delta_S = P_3 L_0/2 = 1.1 \pm 0.1$ nm approximately corresponded to that at 20 °C, thus, confirming the structural temperature stability of the membranes.

In the sample series with the DNDZ+ diamonds, the original matrix at 50 °C had the channels with approximately the same diameter $d_{IC} = (L_0 - 2\delta_S) = 0.5 \pm 0.1$ nm as that at 20 °C (0.52 nm). In the composite material (50 °C), the diameter decreased by $\sim 20\%$ up to $d_{IC} = 0.4 \pm 0.1$ nm under the influence of the DNDZ+ diamonds ($C = 5$ wt.%).

When composite materials with DNDZ- were heated to 50 °C, the correlation pattern between $\kappa_N^{1/2}$ and L_N was retained. With $C = 1-5$ wt.%, $\kappa_N^{1/2} = P_2(L_N - P_3)$ with $P_2 = 4.42 \pm 0.01$, $P_3 = 0.763 \pm 0.001$ was observed due to the channel diameter variation (Figure 7, *b*). Channel shell thickness $\delta_S = P_3 L_0/2 = 1.04 \pm 0.01$ nm was comparable with that in composite materials with DNDZ+. Channel diameter in the heated matrix was $d_I = L_0 - 2\delta_S = 0.64 \pm 0.01$ nm, and saturation with the DNDZ-diamonds ($C = 5$ wt.%) gave rise to channel compression by $\sim 14\%$ to $d_I = 0.55 \pm 0.02$ nm.

Review of the structural examination and membrane conductometry data in the initial and heated conditions has identified common patterns of the channel structure influence on the ion conductivity of the sample series with diamonds (DNDZ+, DNDZ-) with low and high diamond content (0.25–0.5, 1–5 wt.%). Channel assembly compaction and channel compression prevailed in the first and second ranges, respectively. The first mode is typical of the DNDZ+ diamonds due to their attraction to the

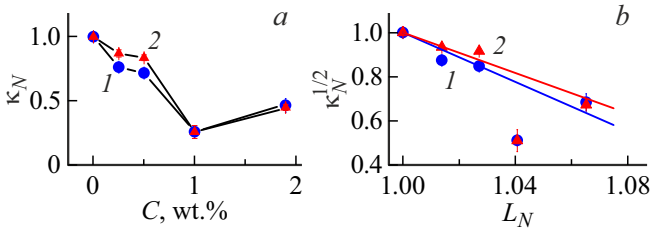

Figure 8. Normalized ion conductivity of composite materials κ_N and $\kappa_N^{1/2}$ data (a, b) at 20 and 50 °C $(1, 2)$ depending on the fraction of the DNDF diamonds (C) and channel packaging period (L_N), respectively. Linear data approximation is shown (b).

copolymer ion groups, the second mode is typical of the DNDZ- diamonds due to their repulsion from the groups and segregation trends in the matrix. The analysis has identified the advantages of using the DNDZ+ diamonds with positive surface potential to improve the conductive properties of membranes.

In addition to the matrix modification with hydrophilic diamonds (DNDZ+, DNDZ-), it was interesting to understand the way how hydrophobic diamonds with fluorinated surface affect the matrix structure and proton conductivity [30].

Unlike the DNDZ+ and DNDZ-particles, the DNDF diamonds interact primarily with the hydrophobic skeleton copolymer chains, thus, damaging their packaging. As the matrix gets filled with the DNDF particles, the channel packaging period increases (Figure 2, *d*) leading to a considerable decrease in the ion conductivity (Figure 8, *a*) with the critical concentration $C^* = 1$ wt.%, as in the hydrophilic diamond case.

$\kappa_N^{1/2}$ and L_N demonstrated the linear correlation $\kappa_N^{1/2} = 1 - P_1(L_N - 1)$ with $P_1 = 4.6 \pm 0.5$, $P_1 = 5.6 \pm 0.6$ at 20 and 50 °C (Figure 8, *b*). Increased temperature caused the growth of P_1 by $\sim 20\%$ because polymer chain mobility has increased and diamonds were incorporated between the chains more actively during heating. As the matrix got filled with diamonds, not only loosening of the channel packaging with increasing packaging period (Figure 2, *b*), but also damaged channel coherence were observed. Therefore, the conductivity of composite materials decreased considerably with the fraction of diamonds of $C = 1$ wt.% (Figure 8, *a*), and its partial reduction when the fraction of diamonds grew to 2 wt.% was caused by their segregation when they excited the ion channel network to a lesser extent.

Unlike the carrier groups, the polar groups of DNDZ+ and DNDZ- particles that form chain scaffolds in the matrix to compress the channel assemblies and ion channels, fluorinated diamonds loosen the hydrophobic chain packaging and fragment the channel network, thus, weakening the membrane conductivity considerably. The revealed mechanisms of action of hydrophilic and hydrophobic filler particles on the membrane ion channel network haven't been discussed before. The study was successful in finding the patterns that controlled electrophysical properties of membranes driven not only by the amount of incorporated particles, but also by the surface properties (hydrophilic, hydrophobic), which predetermined the type of interaction between the perfluorinated copolymer and its polar and non-polar fragments.

Conclusion

The neutron scattering experiments in perfluorinated composite membranes with incorporated detonation nanodiamonds identified the type of ion channel ordering with parallel packaging into assemblies with transverse periods set by the external dimensions of polymer channel shells.

In the polymer matrix, the hydrophilic DNDZ+ and DNDZ-diamonds with positive or negative surface potential, due to the presence of functional groups (H, OH or COOH), interacted with polar chain fragments acting directly on the channel network of the membranes.

Small concentrations of modifiers compacted the membrane channel network by reducing the channel packaging periods in the assemblies enclosed by the scaffolds composed of diamond chain aggregates. Due to the electrostatic attraction to the copolymer ion groups, even small amounts of DNDZ+ particles ($C = 0.5$ wt.%) caused the increase in ion conductivity of composite materials at 50 °C with growth by $\sim 30\%$ which was facilitated by hydrogen bonds between the components. In case of similar (negative) charges in the polyelectrolyte and incorporated DNDZ-particles ($C = 0.25$ wt.%), the achieved effect was thrice as low due to the mutual repulsion of components and diamond segregation trends. Membrane enrichment with different diamonds to $C = 5$ wt.% gave rise to ion channel compression by 20% and ion conductivity reduction of the materials.

Unlike the hydrophilic DNDZ+ and DNDZ- particles, primarily hydrophobic DNDF diamonds, incorporated into the matrix, with fluorinated surface contacted with nonpolar copolymer skeleton chains by loosening the copolymer structure, increasing the channel packaging period and fragmenting the channel network, thus causing the fourfold reduction of the material's ion conductivity.

When various diamonds were incorporated into the matrix, general particle size exciting effect on the polymer packaging was observed with the critical concentration $C^* = 1$ wt.%, when the distance between them in the matrix decreased on average to the polymer domain size (~ 20 nm), and copolymer ordering with formation of ion channels was complicated significantly, which reduced the ion conductivity considerably.

In future, the obtained results identifying the mechanisms of influence of the diamond modifier on the structure and ion conductivity of perfluorinated membranes will be used to select the properties and concentrations of diamond particles in a targeted manner to form composite materials

with improved functional properties that are necessary in hydrogen energy, chemical and other technologies.

Funding

This study was supported by the Russian Science Foundation (grant No. 23-23-00129).

Conflict of interest

The authors declare no conflict of interest.

References

[1] J.-H. Kim, S.-K. Kim, K. Nam, D.-W. Kim. J. Membrane Sci., **415**–**416**, 696 (2012). DOI: 10.1016/j.memsci.2012.05.057
[2] K. Li, G. Ye, J. Pan, H. Zhang, M. Pan. J. Membrane Sci., **347** (1−2), (2010). https://doi.org/10.1016/j.memsci.2009.10.002
[3] D. Choi. Membranes, **12**, 680 (2022). https://doi.org/10.3390/membranes12070680
[4] A.K. Sahu, S. Pitchumani, P. Sridhar, A.K. Shukla. Bull. Mater. Sci., **32** (3), 285 (2009).
[5] A.C. Brown, J.J. Hargreaves. Green Chem., **1** (1), 17 (1999).
[6] Y. Lu, Y. Yang, A. Sellinger, M. Lu, J. Huang, H. Fan, R. Haddad, G. Lopez, A.R. Burns, D.Y. Sasaki. Nature, **410** (6831), 913 (2001).
[7] T. Hao-lin, P. Mu, M. Shi-chun, Y. Run-zhang. J. Wuhan Univ. Technol.-Mat. Sci. Edit., **19**, 7 (2004). https://doi.org/10.1007/BF02835048
[8] N.H. Jalani, K. Dunn, R. Datta. Electrochim. Acta, **51** (3), 553 (2005).
[9] E. Chalkova, M.B. Pague, M.V. Fedkin, D.J. Wesolowski, S.N. Lvov. J. Electrochem. Society, **152** (6), A1035 (2005).
[10] K.T. Adjemian, R. Dominey, L. Krishnan, H. Ota, P. Majsztrik, T. Zhang, J. Mann, B. Kirby, L. Gatto, M. Velo-Simpson. Chem. Mater., **18** (9), 2238 (2006).
[11] Z. Chen, B. Holmberg, W. Li, X. Wang, W. Deng, R. Munoz, Y. Yan. Chem. Mater., **18** (24), 5669 (2006).
[12] S. Licoccia, E. Traversa. J. Power Sources, **159** (1), 12 (2006).
[13] S. Simonov, M.S. Kondratenko, I.V. Elmanovich, V.E. Sizov, E.P. Kharitonova, S.S. Abramchuk, A.Yu. Nikolaev, D.A. Fedosov, M.O. Gallyamov, A.R. Khokhlov. J. Membr. Sci., **564**, 106 (2018). https://doi.org/10.1016/j.memsci.2018.06.042
[14] T. Hao-lin, P. Mu, M. Shi-Chun, Y. Run-Zhang. Chin. J. Inorg. Chem., **20** (2), 128 (2004).
[15] M.A. Zulfikar, A.W. Mohammad, N. Hilal. Desalination, **192** (1−3), 262 (2006).
[16] W. Jia, K. Feng, B. Tang, P. Wu. J. Mater. Chem. A, **3**, 15607 (2015). https://doi.org/10.1039/C5TA03381K
[17] S. Lu, D. Wang, S.P. Jiang, Y. Xiang, J. Lu, J. Zeng. Adv. Mater., **22** (9), 971 (2010).
[18] C.-C. Yang, Y.J. Li, T.-H. Liou. Desalination, **276** (1), 366 (2011).
[19] Sujie Xing, He Xu, Junshui Chen, Guoyue Shi, Litong Jin. J. Electroanal. Chem., **652** (1−2), 60 (2011).
[20] M.R.H. Siddiqui, A.I. Al-Wassil, A.M. Al-Otaibi, R.M. Mahfouz. Mater. Res., **15** (6), 986 (2012).
[21] S. Liu, J. Yu, Y. Hao, F. Gao, M. Zhou, L. Zhao. Hindawi Intern. J. Polym. Sci., **2024**, 630992 (2024). https://doi.org/10.1155/2024/6309923
[22] D. Yuan, Z. Liu, S.W. Tay, X. Fan, X. Zhang, C. He. Chem. Commun., **49**, 9639 (2013). https://doi.org/10.1039/C3CC45138K
[23] A.H. Tian, J.-Y. Kim, J.Y. Shi, K. Kim, K. Lee. J. Power Sour., **167**, 302 (2007). https://doi.org/10.1016/j.jpowsour.2007.02.074
[24] M.V. Lebedeva, A.V. Ragutkin, A.P. Antropov, N.A. Yashtulov. IOP Conf. Series: Mater. Sci. Engineer., **744**, 012007 (2020). DOI: 10.1088/1757-899X/744/1/012007
[25] R. Singwadi, M. Dhlamini, T. Mokrani, F. Nemavhola. Digest J. Nanomater. Biostructures, **12** (4), 1137 (2017).
[26] Z. Chen, B. Holmberg, W. Li, X. Wang, W. Deng, R. Munoz, Y. Yan. Chem. Mater., **18** (24), 5669 (2006).
[27] E.N. Karaulova, E.I. Bagry. Usp. khim., **68**, 11 (979). (in Russian). DOI: https://doi.org/10.1070/RC1999v068n11ABEH000499
[28] T.P. Dyachkova, A.G. Tkachev *Metody funktsionalizatsii i modifitsirobaniya uglerodnykh nanotrubok* (Izdat dom Spektr, M., 2013) 152 s. ISBN 978-5-4442-0050-6 (in Russian).
[29] A.E. Aleksenskii. *Thechnology of preparation of detonation nanodiamond*, in A.Y. Vul, O.A. Shenderova (ed). *Detonation nanodiamonds. Science and Applications* (Pan Stanford Publishing: Danvers, MA, USA, 2014), p. 37–72.
[30] A. Aleksenskii, M. Bleuel, A. Bosak, A. Chumakova, A. Dideikin, M. Dubois, E. Korobkina, E. Lychagin, A. Muzychka, G. Nekhaev et al. Nanomaterials, **11**, 1945 (2021).
[31] O.V. Tomchuk, V. Ryukhtin, O. Ivankov, A.Ya. Vul, A.E. Aleksenskii, L.A. Bulavin. Fuller. Nanotub. Carbon Nanostructur., **28**, 272 (2020).
[32] A.V. Petrov, K.N. Semenov, I.V. Murin. Russ. J. Gen. Chem., **90**, 927 (2020).
[33] I.I. Kulakova, G.V. Lisichkin. ZhOKh, **90** (10), 1601 (2020) (in Russian) DOI: 10.31857/S0044460X20100157
[34] D. Chen, H. Feng, J. Li. Chem. Rev., **112** (11), 6027 (2012). https://doi.org/10.1021/cr300115g
[35] D.V. Postnov, N.A. Melnikova, V.N. Postnov, K.N. Semenov, I.V. Murin. Rev. Adv. Mater. Sci., **39**, 20 (2014).
[36] S.F. Nitodas, M. Das, R. Shah. Membranes, **12**, 454 (2022). https://doi.org/10.3390/membranes12050454
[37] V.N. Postnov, N.A. Melnikova, G.A. Shulmeister, A.G. Novikov, I.V. Murin, A.N. Zhukov. Russ. J. Gen. Chem., **87**, 2754 (2017).
[38] A.B. Yaroslavtsev, I.A. Stenina. Mendeleev Commun., **31**, 423 (2021).
[39] A.B. Yaroslavtsev, I.A. Stenina, D.V. Golubenko. Pure Appl. Chem., **92**, 1147 (2020).
[40] O.N. Primachenko, Yu.V. Kulvelis, V.T. Lebedev, A.S. Odinokov, V.Yu. Bayramukov, E.A. Marinenko, I.V. Gofman, A.V. Shvidchenko, A.Ya. Vul, S.S. Ivanchev. Membranes Membrane Technol., **2** (1), 1 (2020).
[41] Y.-L. Liu, Y.-H. Su, C.-M. Chang, Suryani, D.-M. Wang, J.-Y. Lai. J. Mater. Chem., **20**, 4409 (2010). https://doi.org/10.1039/C000099J
[42] M.S. Asgari, M. Nikazar, P. Molla-abbasi, M.M. Hasani-Sadrabadi. Intern. J. Hydrogen Energy, **38** (14), 5894 (2013). https://doi.org/10.1016/j.ijhydene.2013.03.010
[43] A.O. Krasnova, N.V. Glebova, A.G. Kastsova, M.K. Rabchinskii, A.A. Nechitailov. Polymers (Basel), **15** (9), 2070 (2023). DOI: 10.3390/polym15092070
[44] M. Vinothkannan, A.R. Kim, G. Gnana kumar, D.J. Yoo. RSC Adv., **8**, 7494 (2018). https://doi.org/10.1039/C7RA12768E.

[45] M. Vinothkannan, A.R. Kim, D.J. Yoo. RSC Adv., **11**, 18351 (2021). DOI: 10.1039/D1RA00685A.
[46] A.V. Shvidchenko, A.S. Odinokov, O.N. Primachenko, I.V. Gofman, N.P. Yevlampieva, E.A. Marinenko, V.T. Lebedev, A.I. Kuklin, Y.V. Kulvelis. Membranes, **13**, 712 (2023). https://doi.org/10.3390/membranes13080712
[47] Yu.V. Kulvelis, O.N. Primachenko, I.F. Gofman, A.S. Odinokov, A.V. Shvidchenko, E.B. Yudina, E.A. Marinenko, V.T. Lebedev, A.Ya. Vul'. Izv. AN, ser. khim. **9**, 1713 (2021) (in Russian).
[48] O.N. Primachenko, E.A. Marinenko, A.S. Odinokov, S.V. Kononova, Yu.V. Kulvelis, V.T. Lebedev. Polymer. Adv. Technol., **32** (4), 1386 (2021). https://doi.org/10.1002/pat.5191
[49] W.Y. Hsu, T.D. Gierke. J. Membr. Sci., **13**, 307 (1983).
[50] A. Eisenberg. Macromolecules, **3**, 147 (1970). https://doi.org/10. 1021/ma60014a006
[51] A. Eisenberg, B. Hird, R.B. Moore. Macromolecules, **23**, 4098 (1990). https://doi.org/10.1021/ma00220a012
[52] M. Fujimura, T. Hashimoto, H. Kawai. Macromolecules, **15**, 136 (1982). https://doi.org/10.1021/ma00229a028
[53] G. Gebel. Macromolecules, **33**, 4850 (2000). https://doi.org/10.1021/ma9912709
[54] A.-L. Rollet, O. Diat, G. Gebel. J. Phys. Chem. B, **106**, 3033 (2002). https://doi.org/10.1021/jp020245t
[55] L. Rubatat, G. Gebel, O. Diat. Macromolecules, **37**, 7772 (2004). https://doi.org/10.1021/ma049683j
[56] G. Gebel, O. Diat. Fuel Cells, **5**, 261 (2005). https://doi.org/10.1002/fuce200400080
[57] M.H. Kim, C.J. Glinka, S.A. Grot, W.G. Grot. Macromolecules, **39**, 4775 (2006). https://doi.org/10.1021/ma060576u
[58] K. Schmidt-Rohr, Q. Chen. Nat Mater., **7**, 75 (2008). https://doi. org/10.1038/nmat2074
[59] K.-D. Kreuer. Chem. Mater., **26**, 361 (2014). https://doi. org/10.1021/cm402742u
[60] K.-D. Kreuer, G. Portale. Adv. Funct. Mater., **23**, 5390 (2013). https://doi.org/10.1002/adfm.201300376
[61] J.A. Elliott, D. Wu, S.J. Paddison, R.B. Moore. Soft Matter., **7**, 6820 (2011). https://doi.org/10.1039/c1sm00002k
[62] V.T. Lebedev, Yu.V. Kulvelis, A.V. Shvidchenko, O.N. Primachenko, A.S. Odinokov, E.A. Marinenko, A.I. Kuklin, O.I. Ivankov. Membranes, **13**, 850 (2023). https://doi.org/10.3390/membranes13110850
[63] O.N. Primachenko, A.S. Odinokov, E.A. Marinenko, Yu.V. Kulvelis, V.G. Barabanov, S.V. Kononova. J. Fluor. Chem., **244**, 109736 (2021). http://doi.org/10.1016/j.jfluchem.2021.109736
[64] O. Williams, J. Hees, C. Dieker, W. Jager, L. Kirste, C.E. Nebel. ACS Nano, **4**, 4824 (2010).
[65] A.E. Aleksenskii, E.D. Eydelman, A.Ya. Vul. Nanotechnol. Lett., **3**, 68 (2011).
[66] A.Ya. Vul, A.T. Dideikin, A.E. Aleksenskiy, M.V. Baidakova. *Detonation nanodiamonds. Synthesis, properties and applications*, in: O.A. Williams (ed), *Nanodiamond, RSC Nanoscience and Nanotechnology* (Thomas Graham House, Science Park, Milton Road, Cambridge CB4 0WF, UK, 2014)
[67] A. Aleksenskii, M. Bleuel, A. Bosak, A. Chumakova, A. Dideikin, M. Dubois, E. Korobkina, E. Lychagin, A. Muzychka, G. Nekhaev et al. Nanomaterials, **11**, 3067 (2021). https://doi.org/10.3390/nano11113067
[68] V.V. Nesvizhevsky, U. Koester, M.Dubois, N. Batisse, L. Frezet, A. Bosak, L. Gines, O. Williams. Carbon, **130**, 799 (2018).
[69] O.N. Primachenko, A.S.Odinokov, V.G. Barabanov, V.P. Tyulmankov, E.A. Marinenko, I.V. Gofman, S.S. Ivanchev. ZhPKh, **91**, 110 (2018) (in Russian).
[70] A.I. Kuklin, A.I. Ivankov, D.V. Soloviov, A.V. Rogachev, Y.S. Kovalev, A.G. Soloviev, A.K. Islamov, M. Balasoiu, A.V. Vlasov, S.A. Kutuzov. J. Phys. Conf. Ser., **994**, 012016 (2018). http://doi.org/10.1088/1742-6596/994/1/012016
[71] A.I. Kuklin, O.I. Ivankov, A.V. Rogachev, D.V. Soloviov, A.Kh. Islamov, V.V. Skoi, Yu.S. Kovalev, A.V. Vlasov, Yu.L. Ryzhykau, A.G. Soloviev, N. Kucerka, V.I. Gordeliy. Crystallogr. Rep., **66**, 231 (2021). http://doi.org/10.1134/S1063774521020085
[72] A.G. Soloviev, T.M. Solovjeva, O.I. Ivankov, D.V. Soloviov, A.V. Rogachev, A.I. Kuklin. J. Phys.: Conf. Ser., **848**, 012020 (2017). https://doi.org/10.1088/1742-6596/848/1/012020
[73] D.I. Svergun, L.A. Feigin. *Structure Analysis by Small-Angle X-Ray and Neutron Scattering* (Plenum Press, NY. & London, 1987)
[74] O.V. Tomchuk, D.S. Volkov, L.A. Bulavin, A.V. Rogachev, M.A. Proskurnin, M.V. Korobov, M.V. Avdeev. J. Phys. Chem. C, **119**, 794 (2015).
[75] V.T. Lebedev, Yu.V. Kulvelis, A.I. Kuklin, A.Ya. Vul. Condens. Matter., **1** (10), 1 (2016). DOI: 10.3390/condmat1010010
[76] O.N. Primachenko, Yu.V. Kulvelis, A.S. Odinokov, N.V. Glebova, A.O. Krasnova, L.A. Antokolskiy, A.A. Nechitailov, A.V. Shvidchenko, I.V. Gofman, E.A. Marinenko, N.P. Yevlampieva, V.T. Lebedev, A.I. Kuklin. Membranes, **12** (9), 827 (2022). https://doi.org/10.3390/membranes12090827

Translated by E.Ilinskaya